Ghost imaging with thermal light by third-order correlation

Yanfeng Bai and Shensheng Han
Key Laboratory for Quantum Optics and Center for Cold Atom Physics, Shanghai Institute of Optics and Fine Mechanics, Chinese Academy of Sciences, Shanghai 201800, China
(Received 19 July 2007; published 18 October 2007)

Ghost imaging with classical incoherent light by third-order correlation is investigated. We discuss the similarities and the differences between ghost imaging by third-order correlation and by second-order correlation, and analyze the effect from each correlation part of the third-order correlation function on the imaging process. It is shown that the third-order correlated imaging includes richer correlated imaging effects than the second-order correlated one, while the imaging information originates mainly from the correlation of the intensity fluctuations between the test detector and each reference detector, as does ghost imaging by second-order correlation.

DOI: 10.1103/PhysRevA.76.043828 PACS number(s): 42.50.Dv, 42.50.Ar

I. INTRODUCTION

Correlated imaging has been studied extensively in recent years, both experimentally and theoretically [1–14]. It is a technique to image nonlocally an object by transmitting two correlated beams through a test arm and a reference arm, respectively. By measuring the spatial correlation between the two arms, the image of the object inserted into the test arm can be obtained as a function of the position of the detector in the reference arm. The first two-photon imaging experiment was performed based on the quantum nature of the signal and idler photon pairs from spontaneous parametric down conversion [1]. The experiment led to many interesting studies [2–8] and some debate about whether ghost imaging can be achieved with a classical light source. Bennink *et al.* showed that ghost imaging technique does not require entanglement, and provided an experimental demonstration with a classical source [9]. Our group theoretically studied correlated imaging with incoherent source by using classical statistical optics, based on which we gave a proposal to realize lensless Fourier-transform imaging, and discussed its applicability in x-ray diffraction [10]. Recently, the correlated imaging equation for the classical thermal light source was given, and the macroscopic differences of quantum and classical correlated imaging were shown [11]. Very recently, Ou and Kuang rewrote the Gaussian thin lens equations when another reference arm is considered [12]. Furthermore, the experimental demonstration of two-photon correlated imaging with true thermal light from a hollow cathode lamp was also reported [13].

In previous work about correlated imaging by second-order correlation, one can obtain one image in one place (the reference detector) by measuring the second-order intensity correlation. Then, can more images of an object be reconstructed at different places by considering more higher-order correlation? In this paper, we present the third-order correlated imaging theory. It is shown that the spatial information of an object can be produced at two different places by means of a third-order correlated imaging process. By the analytical results and numerical simulation, the effects from different correlation parts of the third-order correlation function on ghost imaging are investigated, and the similarities and the differences between the third-order correlated imaging and the second-order correlated one are also discussed.

II. THE MODEL AND ANALYTICAL RESULTS

Our imaging system includes three arms (see Fig. 1). The classical thermal light source, usually obtained by illuminating a laser beam into a slowly rotating ground glass [15–17], is divided into three beams, which can be implemented by a combination of two beam splitters. The three beams travel through a test arm and two reference arms, which are characterized by their impulse response functions $h_r(x_r,u_r)$ ($r=1,2,3$). An unknown object is included in the test arm. The detector D_r is used to record the intensity distribution at u_r.

The optical field of the source is represented by $E(x)$. As we know that, in many cases, the field fluctuations of a classical light source can be modeled by a complex circular Gaussian random process with zero mean [18], based on which the second-order correlation function of the source fields can be written as [10]

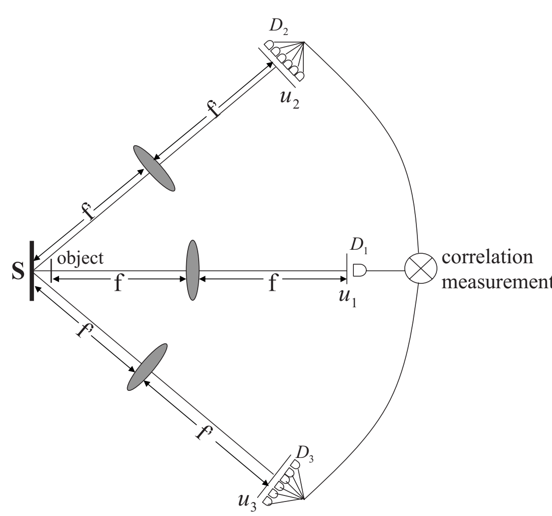

FIG. 1. A scheme for ghost imaging by third-order correlation. The reference arms 2 and 3 are symmetrical about the test arm 1.

 ©2007 The American Physical Society

$$\langle E(x_1)E(x_2)E^*(x_2')E^*(x_1')\rangle = \langle E^*(x_1)E(x_1')\rangle\langle E^*(x_2)E(x_2')\rangle + \langle E^*(x_1)E(x_2')\rangle\langle E^*(x_2)E(x_1')\rangle, \tag{1}$$

where $\langle E^*(x)E(x')\rangle$ is the first-order correlation of the fluctuating source field. From Eq. (1), an arbitrary order correlation function can be expressed via the first-order correlation function. Thus, the third-order correlation function of the source field has

$$\begin{aligned}\langle E^*(x_1)E^*(x_2)E^*(x_3)E(x_1')E(x_2')E(x_3')\rangle = {}& \langle E^*(x_1)E(x_1')\rangle[\langle E^*(x_2)E(x_2')\rangle\langle E^*(x_3)E(x_3')\rangle + \langle E^*(x_2)E(x_3')\rangle\langle E^*(x_3)E(x_2')\rangle] \\ &+ \langle E^*(x_1)E(x_2')\rangle[\langle E^*(x_2)E(x_1')\rangle\langle E^*(x_3)E(x_3')\rangle + \langle E^*(x_2)E(x_3')\rangle\langle E^*(x_3)E(x_1')\rangle] \\ &+ \langle E^*(x_1)E(x_3')\rangle[\langle E^*(x_2)E(x_1')\rangle\langle E^*(x_3)E(x_2')\rangle + \langle E^*(x_2)E(x_2')\rangle\langle E^*(x_3)E(x_1')\rangle].\end{aligned} \tag{2}$$

After propagating through three different optical systems, the field at the detector D_r becomes

$$E_r(u_r) = \int E(x)h_r(x,u_r)dx. \tag{3}$$

The third-order correlation function between the three detectors can be expressed by

$$\begin{aligned}G^{(3)}(u_1,u_2,u_3) &= \langle E^*(u_1)E^*(u_2)E^*(u_3)E(u_1')E(u_2')E(u_3')\rangle \\ &= \int \langle E^*(x_1)E^*(x_2)E^*(x_3)E(x_1')E(x_2')E(x_3')\rangle h_1^*(x_1,u_1)h_1(x_1',u_1) \\ &\quad \times h_2^*(x_2,u_2)h_2(x_2',u_2)h_3^*(x_3,u_3)h_3(x_3',u_3)dx_1dx_1'dx_2dx_2'dx_3dx_3'.\end{aligned} \tag{4}$$

Substituting Eqs. (2) and (3) into Eq. (4), we have

$$\begin{aligned}G^{(3)}(u_1,u_2,u_3) = {}& \langle I_1\rangle\langle I_2\rangle\langle I_3\rangle + \langle I_3\rangle\left|\int dx_1dx_2'\langle E^*(x_1)E(x_2')\rangle h_1^*(x_1,u_1)h_2(x_2',u_2)\right|^2 \\ &+ \langle I_2\rangle\left|\int dx_3dx_1'\langle E^*(x_3)E(x_1')\rangle h_3^*(x_3,u_3)h_1(x_1',u_1)\right|^2 \\ &+ \langle I_1\rangle\left|\int dx_2dx_3'\langle E^*(x_2)E(x_3')\rangle h_2^*(x_2,u_2)h_3(x_3',u_3)\right|^2 \\ &+ \left(\int dx_1dx_2'\langle E^*(x_1)E(x_2')\rangle h_1^*(x_1,u_1)h_2(x_2',u_2)\int dx_2dx_3'\langle E^*(x_2)E(x_3')\rangle h_2^*(x_2,u_2)h_3(x_3',u_3)\right. \\ &\left.\times\int dx_3dx_1'\langle E^*(x_3)E(x_1')\rangle h_3^*(x_3,u_3)h_1(x_1',u_1) + \text{c.c.}\right),\end{aligned} \tag{5}$$

where $\langle I_r\rangle = \langle I(u_r)\rangle$. The first term on the right-hand side of Eq. (5) is the multiplication of the intensity distribution at the three detectors. It contributes only the background, and cannot be used to realize the correlated imaging. The second term is the multiplication between the intensity distribution at the detector D_3 and the intensity fluctuation correlation between the detectors D_1 and D_2, which gives the information of the object imaged at D_2. From the third term, we can obtain the imaging signal at the detector D_3. The fourth term is the correlation of the intensity fluctuations at D_2 and D_3, and the last term is the intensity fluctuation correlation between the three detectors. In the following we will discuss the effect of each correlation part on ghost imaging and will compare our results with those in the second-order correlated imaging.

III. NUMERICAL RESULTS

Suppose the light source is fully spatially incoherent, and its intensity distribution is of the Gaussian type. Then the first-order correlation function for the source can be written as

$$\langle E^*(x)E(x')\rangle = G_0 \exp\left(-\frac{x^2+x'^2}{4a^2}\right)\delta(x-x'), \tag{6}$$

where G_0 is a normalized constant, a is the transverse size of the source.

Now we use the third-order correlation theory to analyze the $2f$ imaging scheme. The test arm consists of an object with transmission function $t(x)$, a lens, and a detector D_1.

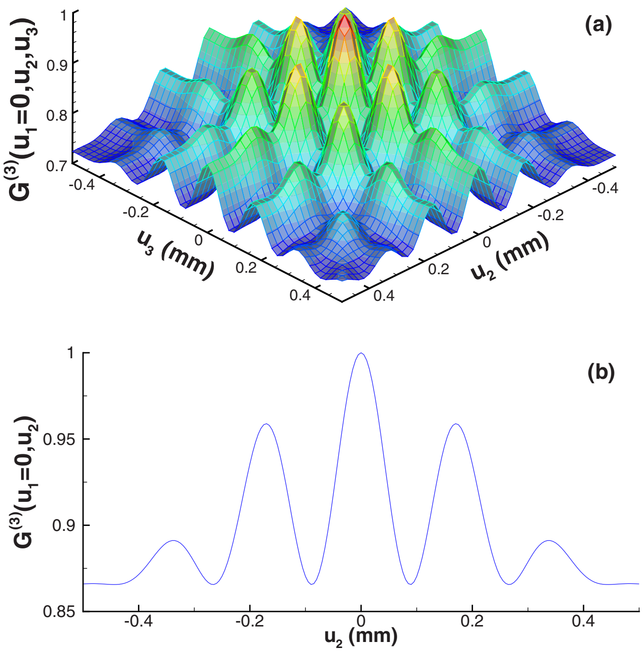

FIG. 2. (Color online) (a) Normalized third-order interference-diffraction pattern at the planes of the reference detectors D_2 and D_3. (b) Normalized $G^{(2)}(u_1=0,u_2)$ for ghost imaging by second-order correlation.

The lens is located at a focal distance f from the object and from D_1. If the size of the lens is much larger than the object, the impulse response function has the form

$$h_1(x_1,u_1) = -\frac{i}{\lambda f} t(x_1) \exp\left(-\frac{i2\pi}{\lambda f} x_1 u_1\right). \tag{7}$$

The two reference arms are identical: a lens is placed at a focal distance f' both from the source and from the detector D_k $(k=2,3)$. For simplicity, we assume $f=f'$. The corresponding impulse response function is

$$h_k(x_k,u_k) = -\frac{i}{\lambda f} \exp\left(-\frac{i2\pi}{\lambda f} x_k u_k\right). \tag{8}$$

Here we take a double slit with the slit width $\omega = 0.075$ mm and the distance between two slits $d = 0.15$ mm as the object imaged. The transverse size of the source $a=1$ mm, other parameters are chosen as $\lambda = 532$ nm, $f=75$ mm.

By using a pointlike test detector located at $u_1=0$ and substituting Eqs. (6)–(8) into Eq. (5), the conditional third-order correlation function $G^{(3)}(u_1=0,u_2,u_3)$ can be obtained. Figure 2(a) shows the simulation result, which is normalized by $G^{(3)}_{\max}$. It clearly emerges that the Fourier-transform image of the double slit can be observed at two different places, the reference detectors D_2 and D_3. For the sake of comparison, in Fig. 2(b) we give the numerical simulation about the reconstruction of the Fourier-transform image from the second-order correlated imaging. It is shown that the images given by the third-order correlation consist with that obtained by the second-order correlation. To get a deeper insight into the relationship between the two ghost imaging theories, we first give the expression of the second-order correlation function [8,10],

$$G^{(2)}(u_1,u_2) = \langle I(u_1)\rangle\langle I(u_2)\rangle + \left| \int dx_1 dx_2' \langle E^*(x_1)E(x_2')\rangle h_1^*(x_1,u_1) h_1(x_2',u_2) \right|^2. \tag{9}$$

It is obvious that Eq. (9) is just the first two terms of Eq. (5), which presents the Fourier-transform image of the object at the reference detector D_2. At this point we can say that the third-order correlated imaging includes all information in ghost imaging by second-order correlation. The contribution from the third term of Eq. (5) is similar to that from the second term, it symmetrically gives the information of the object at the reference detector D_3. In Fig. 3, we depict the superposition effects of the first three terms. It is shown that the pattern is almost the same as that in Fig. 2(a) except for slight amplitude difference.

From the above discussion, the intensity fluctuation correlations between the test detector D_1 and the reference detector D_k (k=2,3) are dominant during third-order correlated imaging. The effects from additional correlation parts, in-

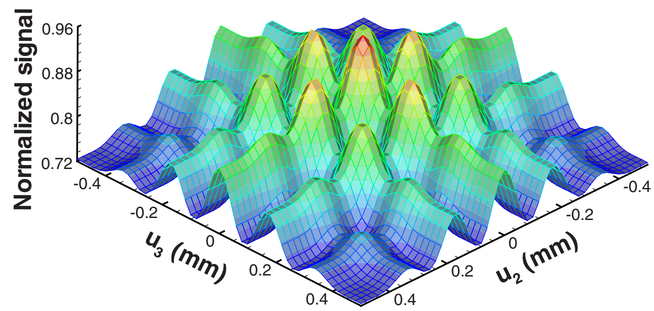

FIG. 3. (Color online) The superposition effects of the background and the intensity fluctuation correlation between the test detector D_1 and the reference detector D_k $(k=2,3)$.

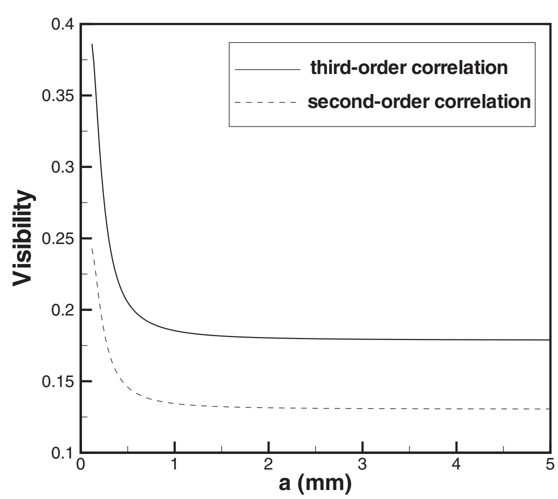

FIG. 4. Dependence of the visibility on the transverse size of the source. Other parameters are the same as those in Fig. 2.

cluding the intensity fluctuation correlations between the two reference detectors and between the three detectors, are quite small, but their existence maybe influenced the visibility of the third-order correlated imaging.

We now investigate the visibility, in previous work it is defined as [19,20]

$$V = \frac{[G^{(2)}(u_1,u_2) - \langle I(u_1)\rangle\langle I(u_2)\rangle]_{\max}}{G^{(2)}(u_1,u_2)_{\max}}. \tag{10}$$

From Ref. [21], we know that the visibility of the object imaged decreases with an increase of the source's transverse size for ghost imaging by second-order correlation. Shown in Fig. 4 is the dependence of the visibility on the transverse size of the source in our imaging system (see the solid line), the dashed line corresponds to the change of the visibility of ghost imaging by second-order correlation. The similarity is that an increase of the transverse size will result in a decrease of the visibility for both cases. The difference between the two curves is induced by the additional correlation parts of Eq. (5), i.e., the correlation of the intensity fluctuations between the two reference detectors and between the three detectors. From Fig. 4 the visibility of third-order correlated imaging is better than that of correlated imaging by second-order correlation.

IV. CONCLUSION

In conclusion, we have investigated the third-order correlated imaging with classical incoherent light. The relationship between ghost imaging by third-order correlation and by second-order correlation is discussed. It is shown that the third-order correlated imaging includes all information of the second-order correlation function. In the process of correlated imaging, the information about the object imaged originates mainly from the intensity fluctuation correlation between the test detector and each reference detector. The additional correlation parts, including the correlation of the intensity fluctuations between the two reference detectors and between all three detectors, only change the amplitude of the imaging signal, i.e., the visibility.

ACKNOWLEDGMENTS

One of the authors (Y.B.) is sincerely grateful to Dr. Hailu Luo for helpful discussions. This research is partly supported by National Natural Science Foundation of China Contract No. 60477007, Shanghai Optical-Tech Special Project Contract No. 034119815, and Shanghai Fundamental Research Project Contract No. 06JC14069.

[1] T. B. Pittman, Y. H. Shih, D. V. Strekalov, and A. V. Sergienko, Phys. Rev. A **52**, R3429 (1995).
[2] D. V. Strekalov, A. V. Sergienko, D. N. Klyshko, and Y. H. Shih, Phys. Rev. Lett. **74**, 3600 (1995).
[3] P. H. S. Ribeiro, S. Padua, J. C. Machado da Silva, and G. A. Barbosa, Phys. Rev. A **49**, 4176 (1994).
[4] A. Gatti, L. A. Lugiato, G. L. Oppo, R. Martin, P. D. Trapani, and A. Berzanskis, Opt. Express **1**, 21 (1997).
[5] P. H. Souto Ribeiro and G. A. Barbosa, Phys. Rev. A **54**, 3489 (1996); P. H. Souto Ribeiro, S. Padua, and C. H. Monken, *ibid.* **60**, 5074 (1999).
[6] B. E. A. Saleh, A. F. Abouraddy, A. V. Sergienko, and M. C. Teich, Phys. Rev. A **62**, 043816 (2000).
[7] A. F. Abouraddy, B. E. A. Saleh, A. V. Sergienko, and M. C. Teich, Phys. Rev. Lett. **87**, 123602 (2001).
[8] A. Gatti, E. Brambilla, and L. A. Lugiato, Phys. Rev. Lett. **90**, 133603 (2003).
[9] R. S. Bennink, S. J. Bentley, and R. W. Boyd, Phys. Rev. Lett. **89**, 113601 (2002).
[10] Jing Cheng and Shensheng Han, Phys. Rev. Lett. **92**, 093903 (2004).
[11] De-Zhong Cao, Jun Xiong, and Kaige Wang, Phys. Rev. A **71**, 013801 (2005).
[12] Li Hua Ou and Leman Kuang, J. Phys. B **40**, 1833 (2007).
[13] D. Zhang, Y. Zhai, L. Wu, and X. Chen, Opt. Lett. **30**, 2354 (2005).
[14] M. Zhang, Q. Wei, X. Shen, Y. Liu, H. Liu, J. Cheng, and S. Han, Phys. Rev. A **75**, 021803(R) (2007).
[15] W. Martienssen and E. Spiller, Am. J. Phys. **32**, 919 (1964).
[16] G. Scarcelli, A. Valencia, and Y. H. Shih, Phys. Rev. A **70**, 051802(R) (2004).
[17] F. Ferri, D. Magatti, A. Gatti, M. Bache, E. Brambilla, and L. A. Lugiato, Phys. Rev. Lett. **94**, 183602 (2005).
[18] J. W. Goodman, *Statistical Optics* (Wiley, New York, 1985).
[19] M. Bache, D. Magatti, F. Ferri, A. Gatti, E. Brambilla, and L. A. Lugiato, Phys. Rev. A **73**, 053802 (2006).
[20] A. Gatti, M. Bache, D. Magatti, E. Brambilla, F. Ferri, and L. A. Lugiato, J. Mod. Opt. **53**, 739 (2006).
[21] Yangjian Cai and Shiyao Zhu, Opt. Lett. **29**, 2716 (2004).